Scientific Research Publishing

Advances in Materials Physics and Chemistry, 2018, 8, 281-294
http://www.scirp.org/journal/ampc
ISSN Online: 2162-5328
ISSN Print: 2162-531X

Determination of Volume Conductivity of Thin Polymeric Films Using Corona Triode, When the Current through the Sample Depends Quadratically on Grid Potential

Pranvera Dhima[1,2], Floran Vila[1]

[1]Department of Physics, University of Tirana, Tirana, Albania
[2]Laboratory of Institute of Communication Technology, University of Technology, Darmstadt, Germany
Email: pranvera_dhima@yahoo.com

How to cite this paper: Dhima, P. and Vila, F. (2018) Determination of Volume Conductivity of Thin Polymeric Films Using Corona Triode, When the Current through the Sample Depends Quadratically on Grid Potential. *Advances in Materials Physics and Chemistry*, **8**, 281-294.
https://doi.org/10.4236/ampc.2018.86019

Received: May 24, 2018
Accepted: June 26, 2018
Published: June 29, 2018

Abstract

In this paper is determined the volume conductivity of thin polymeric films using the corona triode method, when the current through the sample exhibits a quadratic dependence on the grid potential. Based on the experimental data, for the first time, an effective methodology for the determination of volume conductivity, graphically and analytically, is composed. The results obtained by the proposed analytical formula, for polypropylene and Trespaphan, with two different configurations of structures, are closely similar to the graphical method results. In addition, the satisfying accordance of our results, with the results, found out with the consulted literature, obtained by the "static" methods, confirms the accuracy of the proposed methodology, for the determination of volume conductivity of thin polymeric films, using the corona triode.

Keywords

Corona Triode, Polymer Films, Volume Conductivity

1. Introduction

In the last few decades, the application range of thermoplastic polymers has been more and more extended. Their behavior as multifunctional materials, makes them very advantageous over conventional materials. This is the main reason why two of the most widely used among thermoplastic polymers, like polypropylene (PP) and Trespaphan were chosen as objects of our study [1]. Usually, polypropylene films are available in different forms, unoriented, uniaxially

oriented or biaxially oriented, depending upon the desired properties [2].

There are several methods used to determine the volume conductivity of polymers, as an important parameter of their electrical characteristics. In addition to the classic "static" methods (system of electrodes) [3] [4], and the "dynamic" methods, based on electron-beam irradiation effect, in thin polymeric films [5] [6], the corona triode method is used [7].

The experiments show that sample current versus grid potential curves of various polymers, exhibit a linear dependence [7], or power low type dependence [8] [9]. In this work, dealing with the determination of the volume conductivity of thin polymeric films using the corona triode method, results in a quadratic dependence sample current on grid potential. Based on the experimental data, for the first time, an effective methodology for the determination of volume conductivity, graphically and analytically, is composed.

2. Experimental Procedure and Materials

2.1. Measurement Method and Experimental Setup

The samples were corona charged, using the corona triode system (**Figure 1(a)** and **Figure 1(c)**), consisting of a corona electrode, a grounded electrode and a metallic grid inserted between them, to produce a uniform distribution of ions on the sample surface and also to achieve a better control over the potential to which the surface was charged [10] [11].

The distance between the grid and the grounded electrode was 10 mm, while the corona point was positioned at 70 mm over the grid. The corona electrode was energized from a DC high-voltage supply (FUG HCN 14-12500), at 10 kV. Different DC potentials (Model 240 A, Keithley Instruments) of the same polarity as that of the corona electrode were applied to the grid. A digital picoampere meter (Model 445, Keithley Instruments) was used for measuring the sample charging current. The samples were charged for 30 s and immediately after the charging operation, the potential of the charged surface was measured using an electrostatic voltmeter (Model 244, equipped with a probe model 1017), without any physical contact (**Figure 1(b)** and **Figure 1(d)**).

2.2. Materials Tested

The unique combination of its physical, chemical and mechanical properties, enables thermoplastic polymers to be used for an unlimited number of applications.

The first polymer tested, PP, has a semi-crystalline structure, low density of 0.90 g/cm^3, high melting temperature and an excellent chemical resistance [1]. Meanwhile, the second polymer tested Trespaphan (the trade name of biaxially oriented polypropylene (BOPP) [12]), has a regular structure of isotactic polymer chains, an appreciable feature to produce polypropylene thin films [13]. The orientation of molecule chains influences the barrier properties, as well as the mechanical and the optical properties of polymer, improving them [14].

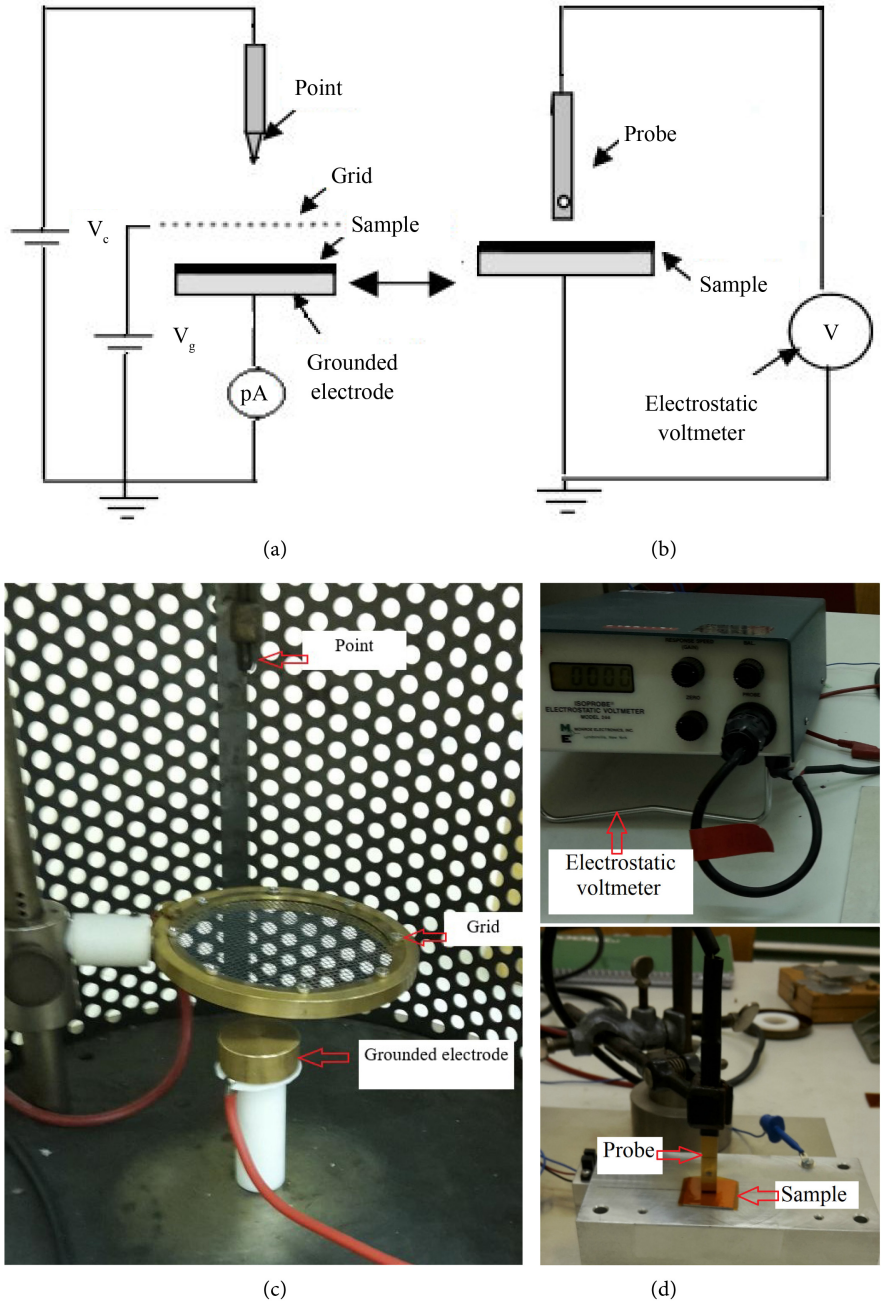

Figure 1. The schematic diagram of the corona triode (a); surface potential measurement scheme (b); corona triode setup (c); electrostatic voltmeter and probe (d).

Therefore, it is preferred for food packaging and meets the specific requirements on health and safety [15]. PP and BOPP films are also used for a wide variety of electrical and electronic applications, including energy storage [1] [16].

PP and Trespaphan samples used in experiments were cut into square sheets of 2.5 cm side length of 50 μm thickness. The accepted dielectric constant (ε) value for both polymers is 2.2. Aluminum foil is attached to the back of the samples to provide a good electrical contact with the grounded electrode on which were laid. We used new samples for each measurement and cleaned them with

isopropanol.

2.3. Experimental Results

The dependencies of the current flowing through the sample and its surface potential, on the grid potential were experimentally studied. Figure 2 and Figure 3, show the corresponding graphs of both of these dependencies, fitted with quadratic and linear functions of the types:

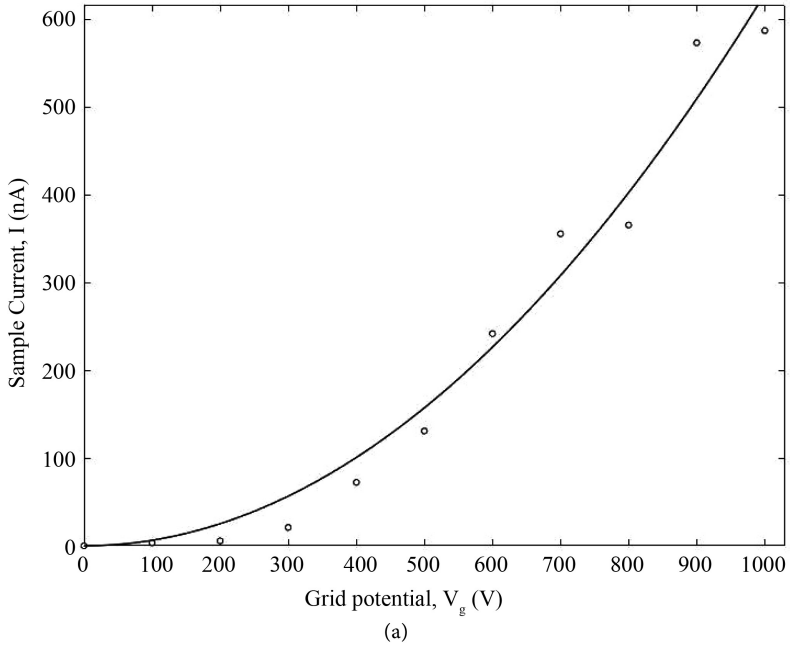

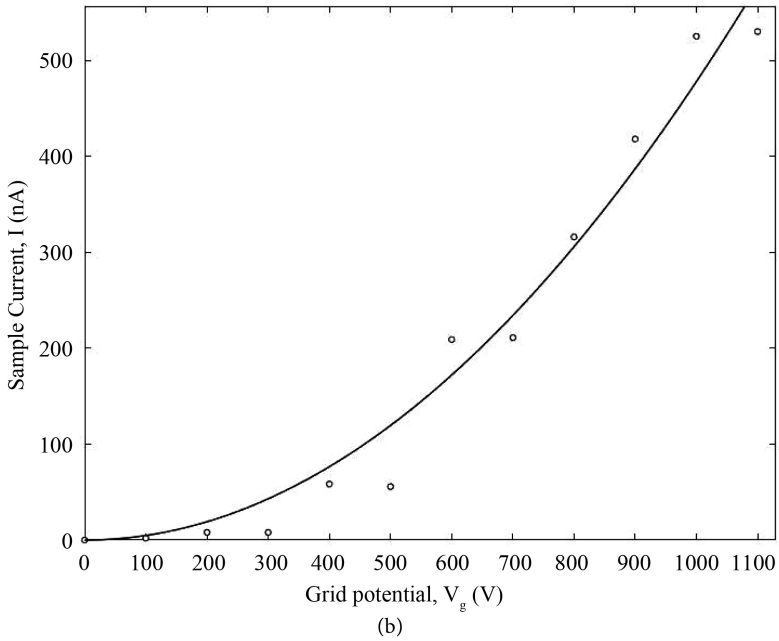

Figure 2. Dependence of the current flowing through the (a) PP and (b) Trespaphan sample, on the grid potential. (The coefficients of determination, R^2, are 0.9749 and 0.9717, respectively).

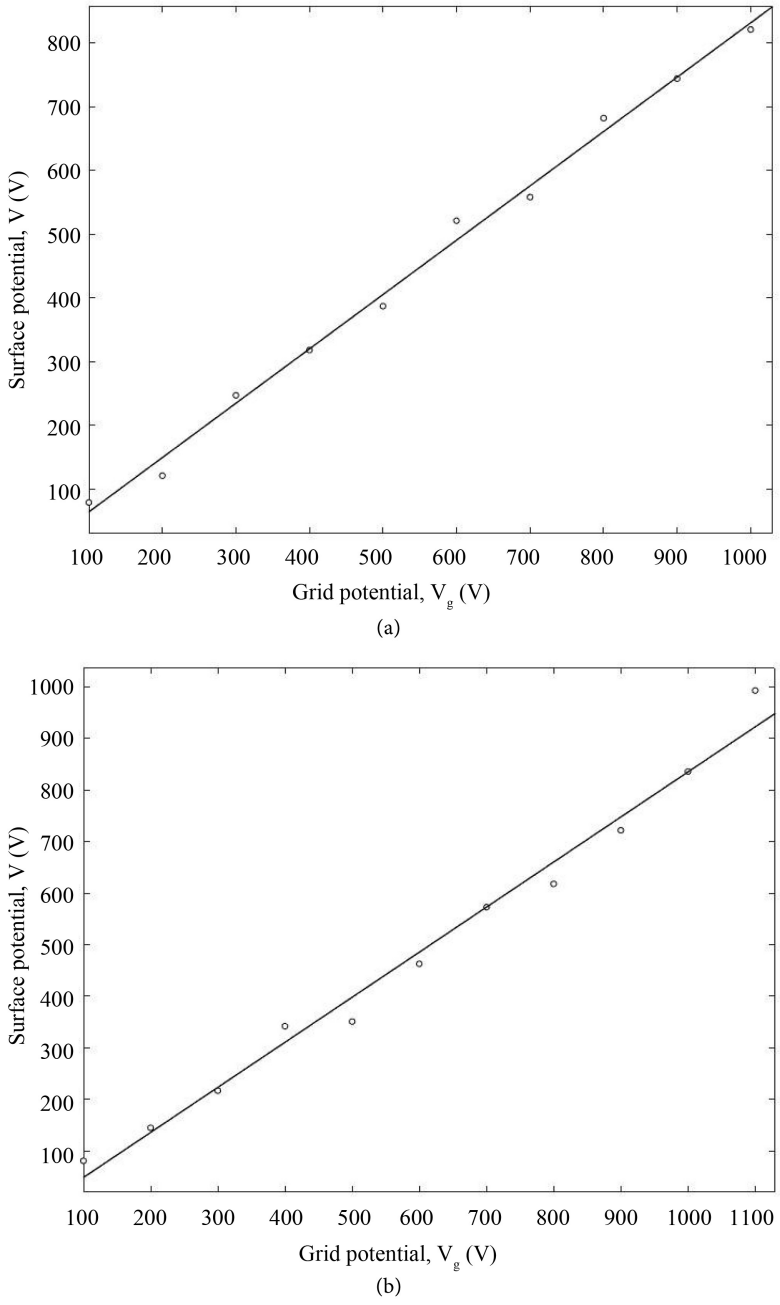

Figure 3. Dependence of the surface potential of (a) PP and (b) Trespaphan sample, on the grid potential. (The coefficients of determination, R^2, are 0.9945 and 0.9856, respectively).

$$I(t) = CV_g^2, \tag{1}$$

and

$$V(0,t) = kV_g - V_0, \tag{2}$$

respectively.

The numerical values of the experimental constants C, k and V_0 can be determined from curves fitting.

3. Determination of Volume Conductivity

The corona triode system, schematically shown in Figure 4, resulted to be very suitable, for the determination of volume conductivity of thin polymeric films. Meanwhile, the relationship between the current intensity $I(t)$, that flows through the sample at a moment of time *t*, and the surface potential $V(0,t)$, caused by that part of positive ions that arrives the sample surface and get trapped, is:

$$\frac{\mathrm{d}}{\mathrm{d}t}V(0,t)+\frac{\gamma}{\varepsilon_0\varepsilon}V(0,t)=\frac{h}{\varepsilon_0 a^2}I(t), \tag{3}$$

where, γ, ε, and h are volume conductivity, dielectric constant and the thickness of the square sample with a length side *a*, respectively [7].

Taking into consideration the fittings of the experimental results from Equation (1) and Equation (2), the differential Equation (3) can be expressed as:

$$\frac{\mathrm{d}}{\mathrm{d}t}V(0,t)+\frac{\gamma}{\varepsilon_0\varepsilon}V(0,t)=\frac{hC_1}{\varepsilon_0 a^2}\left[V(0,t)+V_0\right], \tag{4}$$

where,

$$C_1=\frac{C}{k^2}. \tag{5}$$

If we note:

$$C_2=\frac{\gamma}{\varepsilon_0\varepsilon}; \tag{6}$$

$$C_3=\frac{hC_1}{\varepsilon_0 a^2}, \tag{7}$$

and with the following conditions:

$$\frac{4C_3V_0}{C_2}>1, \tag{8}$$

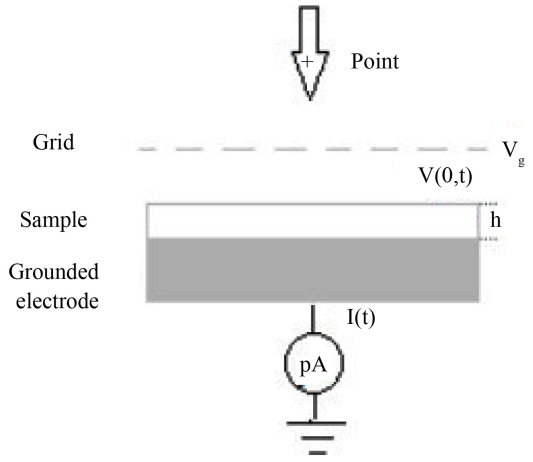

Figure 4. The corona triode scheme (The sample thickness is exaggerated in this figure).

$$\frac{V(0,t)}{V_0} > 1, \tag{9}$$

that are in full agreement with the experimental facts, the solution of the differential Equation (4) can be expressed as:

$$\arctan\left[\left(\frac{V(0,t)+V_0}{V(0,t)-V_0}\right)\sqrt{\frac{4C_3V_0}{C_2}-1}\right] = \pi - \frac{C_2 t}{2}\sqrt{\frac{4C_3V_0}{C_2}-1}. \tag{10}$$

Let us note:

$$\sigma = \frac{V(0,t)+V_0}{V(0,t)-V_0} = \frac{1}{1-\frac{2V_0}{kV_g}}; \tag{11}$$

$$b = 2C_3V_0t; \tag{12}$$

$$x = \sqrt{\frac{4C_3V_0}{C_2}-1}; \tag{13}$$

$$u = \sigma x. \tag{14}$$

Then, the Equation (10), definitely can be expressed as:

$$\arctan u = \pi - \frac{\sigma b u}{\sigma^2 + u^2}. \tag{15}$$

At this moment, u is the unknown quantity. Since the arctan function is defined to lie in the following interval:

$$-\frac{\pi}{2} < \pi - \frac{\sigma b u}{\sigma^2 + u^2} < \frac{\pi}{2}, \tag{16}$$

then, the two graphical solutions of the fundamental Equation (15) lie in the following intervals, respectively:

$$U_1 = \frac{\sigma}{\pi}\left(b - \sqrt{b^2 - \pi^2}\right) < u_1 < \frac{\sigma}{3\pi}\left(b - \sqrt{b^2 - 9\pi^2}\right) = U_2, \tag{17}$$

$$U_2' = \frac{\sigma}{3\pi}\left(b + \sqrt{b^2 - 9\pi^2}\right) < u_2 < \frac{\sigma}{\pi}\left(b + \sqrt{b^2 - \pi^2}\right) = U_1', \tag{17.1}$$

with the condition:

$$b > 3\pi. \tag{18}$$

We emphasize that the two graphical solutions of the Equation (15), will be accepted only if the quantity x, determined by Equation (14), is in full accordance with Equation (8). After determining them numerically, and taking into consideration Equation (13) and Equation (14), we conclude:

$$\gamma = \frac{4\varepsilon_0\varepsilon C_3V_0}{1+x^2}. \tag{19}$$

4. Calculation Results and Analysis

4.1. Experimental Constants

The numerical values of the experimental constants, derived from curves fitting

(Figure 2 and Figure 3) are shown in Table 1.

4.2. Graphical Solutions

Figure 5 demonstrates, for illustration purpose, the two graphical solutions u_1 and u_2 of Equation (15) (the points of intersection between the curves of the functions $y_1 = \arctan u$ and $y_2 = \pi - \frac{\sigma b u}{\sigma^2 + u^2}$), for an average value of grid potentials ($V_g = 500$ V), that lie in the ranges expressed by Equation (17) and Equation (17.1).

Meanwhile, in Table 2, are shown the graphical solutions u_1 and u_2, of Equation (15) (consequently, their corresponding parameters x_1 and x_2, as well), for every grid potential, for PP and Trespaphan.

From Table 2 derive two important features:

Firstly, it can be clearly seen (Figure 6(a) and Figure 6(b)) that the parameter x remains almost constant with σ variation, in full accordance with Equation (14) and with Equations (17) and (17.1) as well.

Secondly, we emphasize that the ensemble of x_1 values, that fulfils the very minimum of the condition (8), is physically unacceptable, because it is in

Table 1. The values of experimental constants obtained from curves fitting for PP and Trespaphan.

Polymer	Experimental Constants					
	$C\left(10^{-13}\Omega^{-1}\cdot V^{-1}\right)$	k	$V_0(V)$	$C_1\left(10^{-13}\Omega^{-1}\cdot V^{-1}\right)$	$C_3\left(10^{-3}V^{-1}\cdot s^{-1}\right)$	b
PP	6.30	0.85	21.1	8.71	7.88	9.98
Trespaphan	4.78	0.87	38.8	6.31	5.71	13.3

Table 2. The graphical solutions of Equation (15) and their corresponding parameters, for PP and Trespaphan.

$V_g(V)$	PP					Trespaphan				
	σ	u_1	x_1	u_2	x_2	σ	u_1	x_1	u_2	x_2
100	1.99	0.566	0.284	11.64	5.85	9.26	1.54	0.166	76.64	8.28
200	1.33	0.401	0.302	7.56	5.68	1.80	0.392	0.218	14.37	7.98
300	1.20	0.367	0.306	6.76	5.63	1.42	0.318	0.224	11.20	7.89
400	1.14	0.351	0.308	6.39	5.61	1.29	0.291	0.226	10.11	7.84
500	1.11	0.342	0.308	6.20	5.59	1.22	0.277	0.227	9.53	7.81
600	1.09	0.337	0.309	6.08	5.58	1.18	0.269	0.228	9.20	7.80
700	1.08	0.334	0.309	6.02	5.57	1.15	0.262	0.228	8.94	7.77
800	1.07	0.332	0.310	5.95	5.56	1.13	0.258	0.228	8.78	7.77
900	1.06	0.329	0.310	5.89	5.56	1.11	0.254	0.229	8.61	7.76
1000	1.05	0.326	0.310	5.83	5.55	1.10	0.252	0.229	8.53	7.75
1100	-	-	-	-	-	1.09	0.250	0.229	8.44	7.74

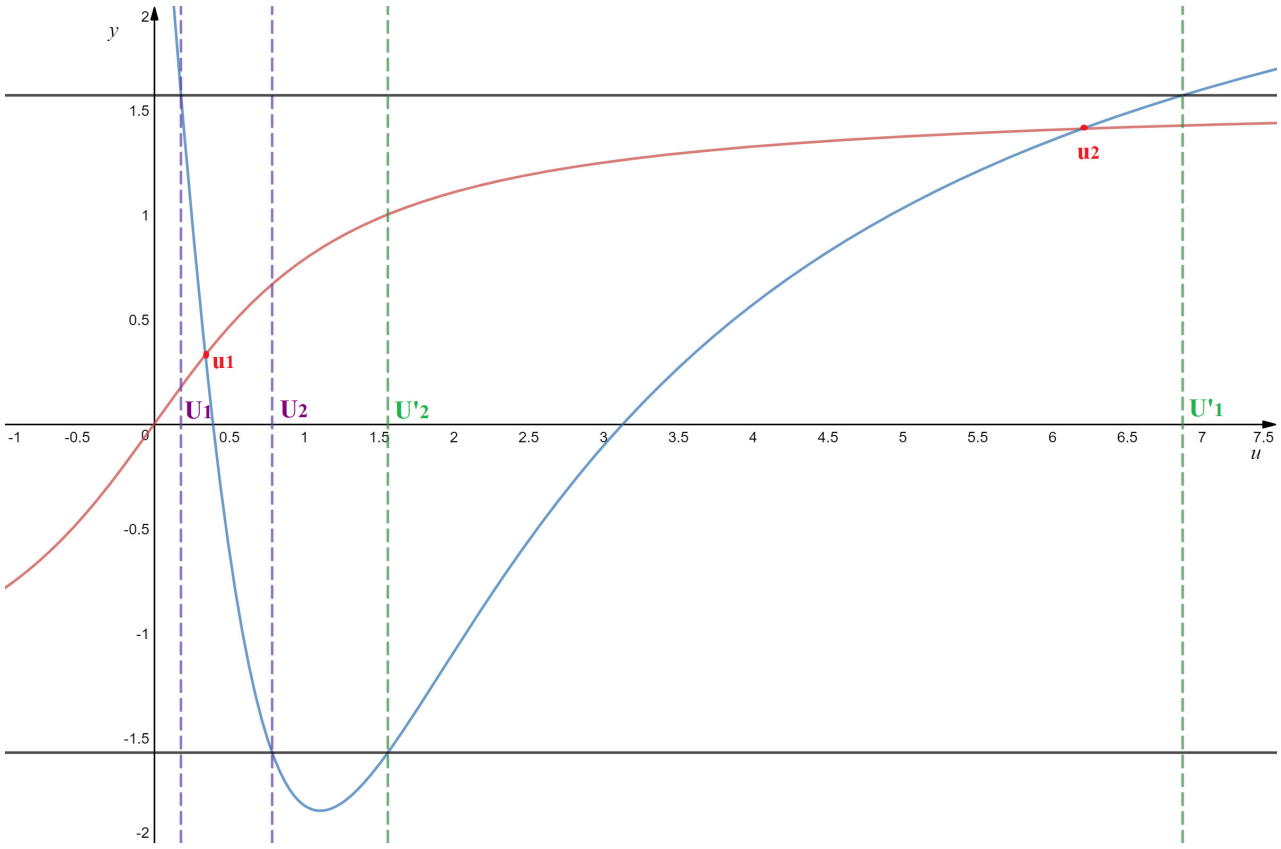

Figure 5. The graphical solutions of the Equation (15) and the intervals where the solutions lie, for PP ($V_g = 500$ V).

contradiction with experimental facts. Therefore, it follows that for determination of volume conductivity by formula (19), only $x = x_2$ should be accepted, that is in full accordance with the physical considerations.

4.3. Analytical Determination of Volume Conductivity

Formula (19) contains constants as well as experimentally determined quantities, except of *x*, that is determined from the graphical solutions u_2 of the Equation (15). But, it would be of great interest, the determination of u_2 (consequently, of *x* and γ, as well) analytically, avoiding the graphical solutions.

The analysis of the experimental facts and the graphical solutions picture (**Figure 7**), show that the values of the parameter *x*, required for the determination of the volume conductivity, can be determined from u_2 solutions that lie in the following range:

$$U_1'' = \frac{3U_1' + U_{02}}{4} < u_2 < U_1', \tag{20}$$

which is included in the interval expressed by Equation (17.1), and:

$$U_{02} = \frac{\sigma}{2\pi}\left(b + \sqrt{b^2 - 4\pi^2}\right), \tag{21}$$

is the point with the greatest value between the two points where the graph of

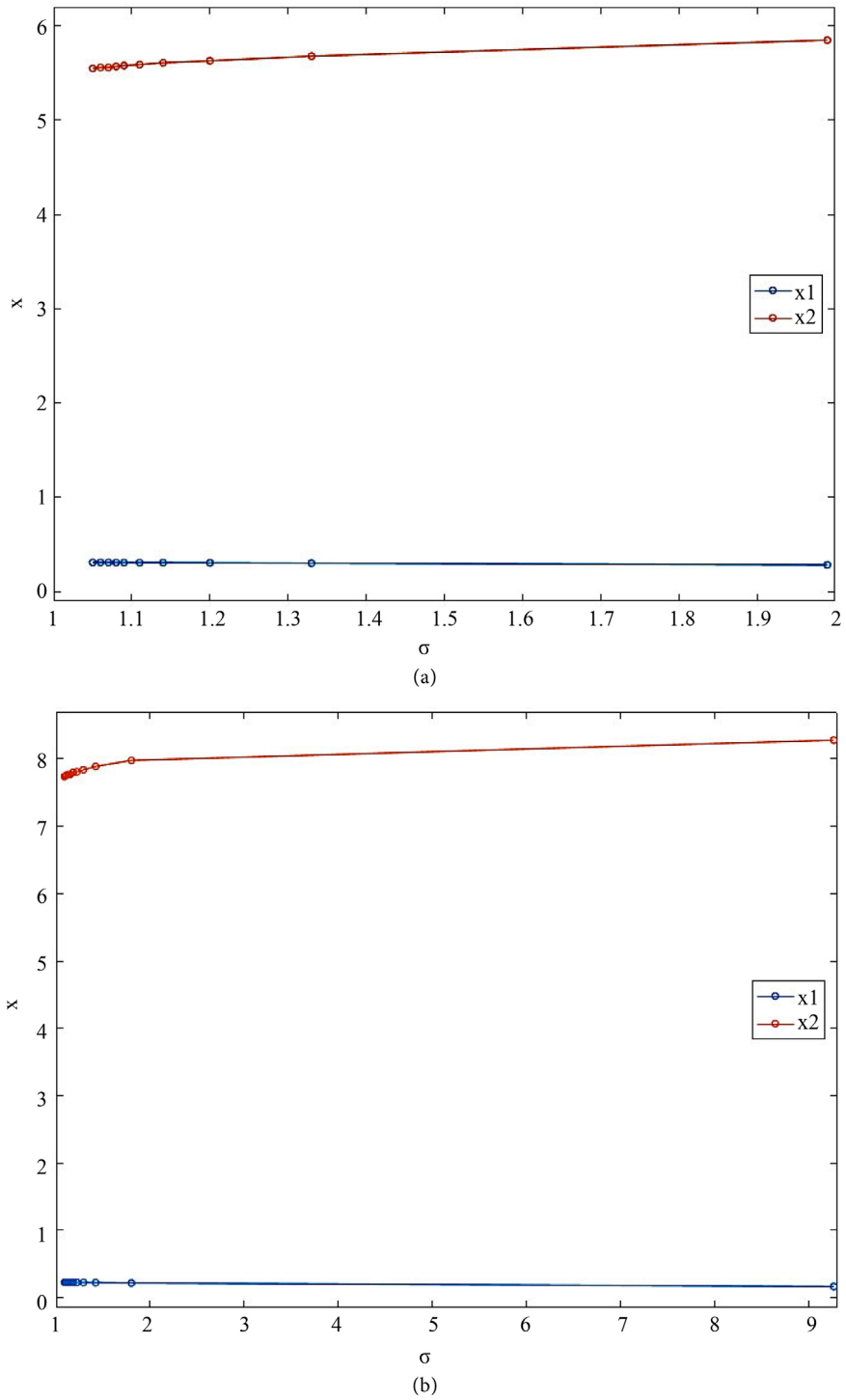

Figure 6. Variation of parameter x with σ, for (a) PP and (b) Trespaphan.

the function y_2 crosses u axis.

Thus, according to Equation (14) and Equation (20) as well, a mean value of x can be determined:

$$\overline{x} = \frac{\delta}{8\pi}, \tag{22}$$

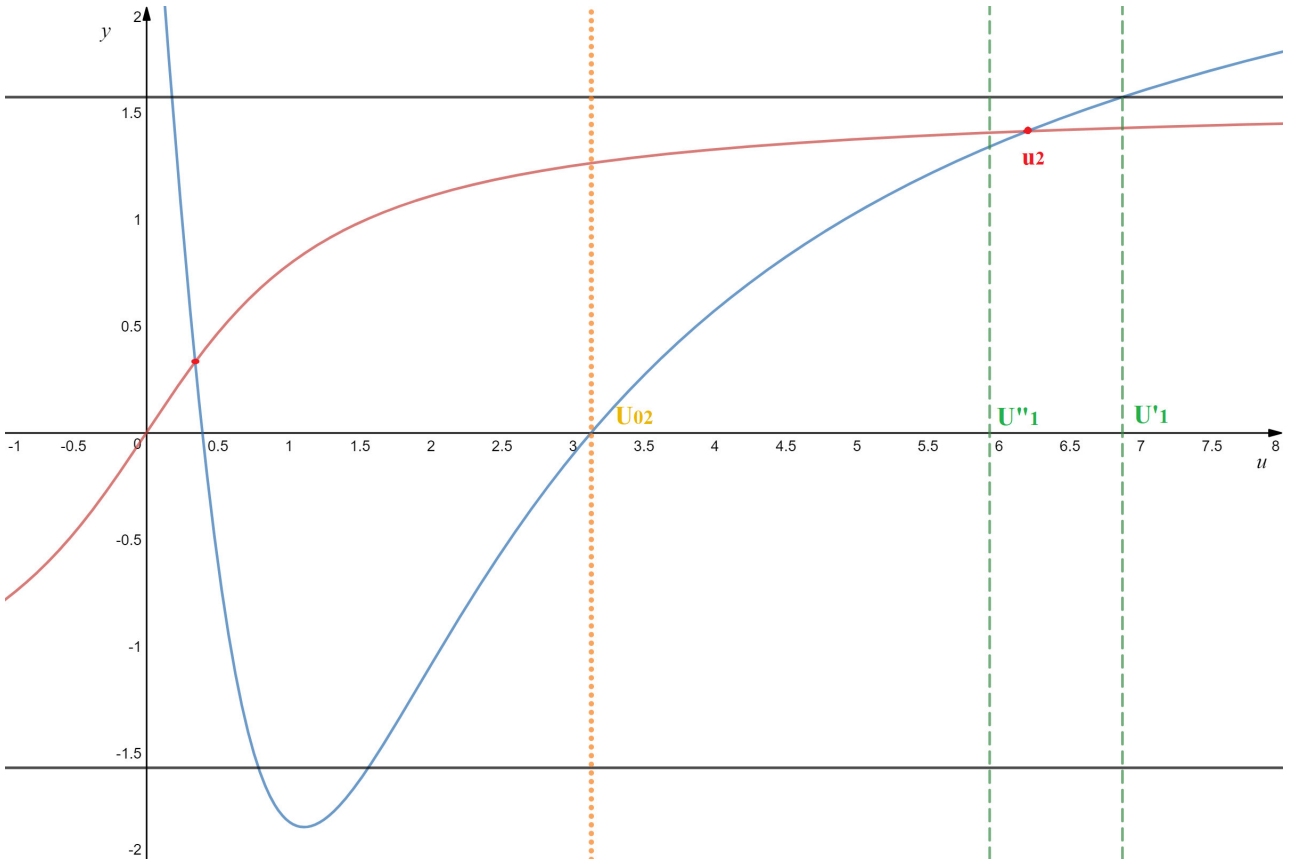

Figure 7. The graphical solution of the Equation (15) and the interval where the accepted solution lies, for PP ($V_g = 500$ V).

where,

$$\delta = 15b\left[1 - \frac{1}{30}\left(\frac{3\pi}{b}\right)^2\right], \tag{23}$$

and definitely, the volume conductivity analytically can be determined by the formula:

$$\gamma = \frac{2\varepsilon_0 \varepsilon b}{\left[1 + \left(\frac{\delta}{8\pi}\right)^2\right] t}. \tag{24}$$

4.4. Numerical Calculation

Let us calculate the value of volume conductivity, by graphical and analytical method.

4.4.1. Graphical Calculation

It is noted that, the experimental constants (**Table 1**) are in full accordance with the conditions expressed by Equation (8), Equation (9) and Equation (18).

The average values of the calculated volume conductivities, according to formula (19), for PP and Trespaphan, and their confidence intervals δ, are

$3.96\times10^{-13}\ \mathrm{S\cdot m^{-1}}$, $2.76\times10^{-13}\ \mathrm{S\cdot m^{-1}}$ and $0.18\times10^{-13}\ \mathrm{S\cdot m^{-1}}$, $0.15\times10^{-13}\ \mathrm{S\cdot m^{-1}}$, respectively. Therefore, the average values of the volume conductivities, determined by graphical method $\overline{\gamma}_g$, lie in the ranges: $3.78\times10^{-13}\ \mathrm{S\cdot m^{-1}} < \overline{\gamma}_g < 4.14\times10^{-13}\ \mathrm{S\cdot m^{-1}}$ and $2.61\times10^{-13}\ \mathrm{S\cdot m^{-1}} < \overline{\gamma}_g < 2.91\times10^{-13}\ \mathrm{S\cdot m^{-1}}$, respectively.

Meanwhile, volume conductivity ranges, for PP and Trespaphan, at the 99% confidence level, are: $3.21\times10^{-13}\ \mathrm{S\cdot m^{-1}} < \gamma_g < 4.71\times10^{-13}\ \mathrm{S\cdot m^{-1}}$ and $2.07\times10^{-13}\ \mathrm{S\cdot m^{-1}} < \gamma_g < 3.45\times10^{-13}\ \mathrm{S\cdot m^{-1}}$, respectively.

4.4.2. Analytical Calculation

The average values of the volume conductivities, calculated according to formula (24), for PP and Trespaphan, are $3.76\times10^{-13}\ \mathrm{S\cdot m^{-1}}$ and $2.79\times10^{-13}\ \mathrm{S\cdot m^{-1}}$, respectively. Volume conductivities values determined by the graphical method, for PP and Trespaphan, have relative errors of 5.0% and 1.1%, respectively, compared with the graphically calculated values. Thus, the intervals of volume conductivities determination, of PP and Trespaphan, are $3.58\times10^{-13}\ \mathrm{S\cdot m^{-1}} < \gamma_a < 3.94\times10^{-13}\ \mathrm{S\cdot m^{-1}}$ and $2.64\times10^{-13}\ \mathrm{S\cdot m^{-1}} < \gamma_a < 2.94\times10^{-13}\ \mathrm{S\cdot m^{-1}}$, respectively.

4.5. Discussion

From the experiments, the volume conductivity of Trespaphan results to be lower than that of PP. But, the two polymers have different orientations of molecule chains, a fact that influences electrical properties. The reason for this may be related to the crystallinity degree, that is increased in biaxially oriented polypropylene films (Trespaphan) compared to unoriented films (PP) [17]. The increase of crystallinity results in the reduce of the conductivity in biaxially oriented polypropylene films [18].

Several studies for PP and Trespaphan, report volume conductivity values of $10^{-13}\ \mathrm{S\cdot m^{-1}}$ order of magnitude [4] [19], meanwhile, in a case, for BOPP films (Trespaphan) a value of $10^{-14}\ \mathrm{S\cdot m^{-1}}$ order of magnitude is also reported [18], found by the "static" methods with various geometrical configurations. The above reported data are considered to be in good agreement with our results, obtained by the corona triode method.

The results obtained for volume conductivity by the graphical method, are closely similar to the analytical method results. This fact shows that the proposed formula (24) allows the determination of volume conductivity of thin polymeric films comfortably and with high accuracy, when the current through the sample exhibits a quadratic dependence on the grid potential.

5. Conclusions

In this paper is determined the volume conductivity of thin polymeric films by the corona triode method, for two polypropylene types, with different orientations of molecule chains.

A special characteristic of the investigated case is the quadratic dependence of

the sample current on the grid potential. For this reason, it is proposed for the first time, a methodology that combines two methods of determination, graphical and analytical, with a high accuracy, as their conductivity ranges largely overlap each other.

The obtained results for volume conductivity, by the proposed methodology, are in good agreement with them obtained by the known "static" methods, and with the theoretical considerations related to the structure of the two types of polypropylene, as well.

References

[1] Maddah, H.A. (2016) Polypropylene as a Promising Plastic: A Review. *American Journal of Polymer Science*, **6**, 1-11.

[2] Massey, K.L. (2004) Film Properties of Plastics and Elastomers: A Guide to Non-oven in Packaging Applications. 2nd Edition, Plastics Design Library/William Andrew Inc., New York, 141.

[3] (1993) Standard Test Methods for DC Resistance or Conductance of Insulating Materials. ASTM Designation D 257-93, 103-119.

[4] Vila, F., Dhima, P. and Mandija, F. (2013) The Influence of Temperature on the Electrical Resistivity of the Cellular Polypropylene and Effect of Activation Energy. *SpringerPlus*, **2**, 472. https://doi.org/10.1186/2193-1801-2-472

[5] Vila, F. and Sessler, G.M. (2001) Influence of Electron Beam Irradiation on Electric Parameters of Dielectric Materials. *Journal of Electrostatics*, **51 & 52**, 146-152. https://doi.org/10.1016/S0304-3886(01)00092-4

[6] Vila, F., Sessler, G.M. and Sykja, H. (2005) The Influence of Electron Beam Irradiation on the Volume Resistivity of Polyethylene and Kapton. *Journal of* Electrostatics, **63**, 749-754. https://doi.org/10.1016/j.elstat.2005.03.039

[7] Dhima, P. and Vila, F. (2017) Determination of Volume Conductivity of Polyethylene Using Positive Corona, When the Current through the Sample Depends Linearly on Grid Potential. *Journal of Materials Science and Chemical Engineering*, **5**, 40-51. https://doi.org/10.4236/msce.2017.512004

[8] Motyl, E. and Kacprzyk, R. (1994) Corona Charging of Polypropylene Films in The Atmosphere of Hydrogen. *Proceedings of the* 8*th International Symposium on Electrets* (*ISE8*), Paris, 7-9 September 1994, 31-36. https://doi.org/10.1109/ISE.1994.514739

[9] Moreno, R.A. and Gross, B. (1976) Measurement of Potential Buildup and Decay, Surface Charge Density and Charging Currents of Corona-Charged Polymer Foil Electrets. *Journal of Applied Physics*, **47**, 3400. https://doi.org/10.1063/1.323199

[10] Giacometti, J.A., Ferreira, G.F. and Gross, B. (1988) A Summary of Corona Charging Methods. *Proceedings of the* 6*th International Symposium on Electrets* (*ISE*6), Oxford, 1-3 September 1988, 87-91. https://doi.org/10.1109/ISE.1988.38528

[11] Giacometti, A. and Oliveira, O.N. (1992) Corona Charging of Polymers. *IEEE Transactions on Electrical Insulation*, **27**, 924-943. https://doi.org/10.1109/14.256470

[12] Ullmann's Editorial Team (2016) Ullmann's Polymers and Plastics, 4 Volume Set: Products and Processes. Volume 1, Wiley Ltd., Hoboken, 1419-1424.

[13] Yard, I.M. (1997) Structure and Properties of Oriented Polymers. 2nd Edition, Springer Science + Business Media, Dordrecht, 435.

[14] Ebnesajjad, S. (2013) Plastic Films for Food Packaging. In: Fereydoon, M. and Ebnesajjad, S., Eds., *Development of High-Barrier Film for Food Packaging*, Elsevier Inc., Oxford, 71.

[15] Bosch, D. (2007) TUV Rheinland LGA, Products. GmbH, Nuremberg.

[16] Chung, T.C.M. (2012) Functionalization of Polypropylene with High Dielectric Properties: Applications in Electric Energy Storage. *Green and Sustainable Chemistry*, **2**, 29-37. https://doi.org/10.4236/gsc.2012.22006

[17] Mayer, C. and Calafut, T. (1998) Polypropylene: The Definitive User's Guide and Databook. Plastics Design Library, New York, 16.

[18] Li, H., *et al.* (2013) Electrical Conduction of Metallized BOPP Films Based on Revised Poole-Frenkel Effect. *Journal of Electrostatics*, **71**, 958-962. https://doi.org/10.1016/j.elstat.2013.08.005

[19] Szentes, *et al.* (2012) Electrical Resistivity and Thermal Properties of Compatibilized Multi-Walled Carbon Nanotube/Polypropylene Composites. *eXPRESS Polymer Letters*, **6**, 494-502. https://doi.org/10.3144/expresspolymlett.2012.52